nature geoscience

LETTERS

PUBLISHED ONLINE: 27 SEPTEMBER 2009 | DOI: 10.1038/NGEO640

Rock pulverization at high strain rate near the San Andreas fault

Mai-Linh Doan[1]* and Gérard Gary[2]

In the damage zone around faults, strain is usually localized along fractures, whereas the blocks enclosed by the fractures remain relatively undamaged[1,2]. Some rocks near the San Andreas fault, however, are pervasively pulverized at distances of up to 400 m from the fault's core[3]; intense fragmentation at such distances is rarely observed along other fault zones. Moreover, these rocks preserve their original grain shapes, indicating that they experienced low total strain[3]. Here we use laboratory experiments to show that the intense fragmentation of intact rocks sampled near the San Andreas fault requires high rates of strain (>150 s^{-1}). Our calculations suggest that the combination of the low amount of strain experienced by the pulverized rocks and the high rates of strain indicated by our experiments could be explained by a supershear rupture—a rupture that propagated along the fault at a velocity equal to or greater than that of seismic shear waves.

Northeast of Los Angeles, the Mojave segment of the San Andreas fault shows unusual fault damage. Outcrops have patches of rock finely broken to a scale smaller than the initial grain size of about 1.5 mm; the damage pattern affects mainly crystalline rock that is not extensively weathered, and has only minor clay content[4,5]. Whereas grain comminution and gouge formation are common within the fault core, where much of the strain occurs, intense pulverization so far from the fault core is unexpected. Here we investigate the role of dynamic loading on the pulverization of rocks near the San Andreas fault by carrying out laboratory experiments on rocks sampled near the fault. We then discuss the implications of these results for the physics of earthquakes.

Dynamic pulverization is a process in which stress localization is inhibited, so that the entire medium can be finely fractured[6]. Strain localization is the consequence of an unstable feedback: the largest pre-existing crack within the material is the most favourable for further fracture propagation, and once extended, it becomes even more amenable to further propagation. As a result, this crack extends at the expense of the others. However, at higher loading rates, this localization process may be inhibited. The favoured crack propagates at a finite rate, limited by the P-wave speed of the medium, and cannot accommodate all of the energy provided to the medium. Other fractures can propagate simultaneously and coalesce to produce numerous small fragments. The sample eventually becomes pulverized[6].

Dynamic pulverization has already been considered along faults[7]. However, the theory of Reches and Dewers[7] results in high strain rates for gouge in the fault core, but in much smaller strain rates at several tens of metres away from the core (see Supplementary Discussion). To understand the effect of strain rate on the damage mode, we conducted experiments aimed at understanding the effect of high strain rates on the fragmentation of intact rocks sampled near the pulverized zone of the San Andreas fault (Supplementary Figs S5 and S6). The experiments were carried out using a split Hopkinson pressure bar (SHPB) apparatus[8] in the Laboratoire de Mécanique des Solides of the École Polytechnique, Palaiseau, France. This technique[9] gives average stress, strain and strain rate in the sample for strain rates as large as 2,000 s^{-1}. Details are given in the Methods section.

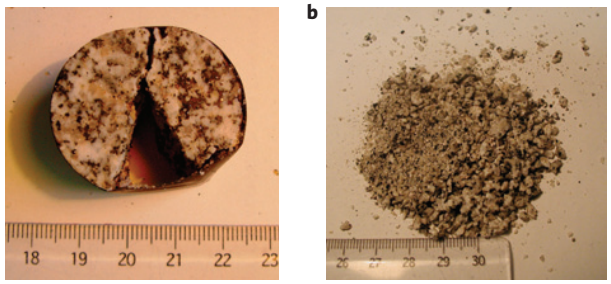

Figure 1 | States of the samples after the experiments. a, At a low strain rate (here, 140 s^{-1}), a rock sample splits into a few fragments when deformed in the SHPB apparatus. **b**, At a higher strain rate (here, 400 s^{-1}), the sample was pulverized into numerous fragments with a diameter smaller than the rock initial grain size. The rulers show centimetres.

Experimental results yielded three types of final state (Figs 1 and 2): (1) an unbroken state, where insufficient loading did not allow the sample to break; (2) a simple fracturing state, where a sample was split by a few (at most three) longitudinal fractures—a common damage pattern for uniaxial loading at low strain rate; and (3) a multiple fragmentation state, when the sample was broken into multiple fragments, some with a size smaller than 1 mm. The experiments carried out at a strain rate higher than 150 s^{-1} produced finely broken samples, whereas those carried out below 100 s^{-1} gave samples broken into two or three fragments (Fig. 2). The interval of strain rate (100 s^{-1}–150 s^{-1}) delimits a transition zone between fracturing and pulverization. In this interval, the maximum stress varies from 50 to 100 MPa, with no clear jump.

We now discuss the pertinence of the laboratory results to explain the natural pulverization. As the tested samples were collected in the damage zone of the San Andreas fault, their Young's modulus is small (10 ± 3 GPa, about one fifth of the tabulated value for granite[10]). The static strength of the material ranges between 50 and 90 MPa, about half the tabulated values for intact granite[11]. These low values suggest that the initial samples were already damaged. This is confirmed by microstructural studies (see the Methods section and Supplementary Figs S7 and S8). All of these cracks competed with the most favourable crack and helped to prevent strain localization along a single fracture. Consequently, we estimate that our threshold strain rate is a minimum value for the transition to fine fragmentation in the field. To verify

[1]Laboratoire de Géophysique Interne et Tectonophysique—CNRS—OSUG, Université Joseph Fourier Grenoble I, BP 53, F-38041 Grenoble, France, [2]Laboratoire de Mécanique des Solides, Ecole Polytechnique, F-91128 Palaiseau, France. *e-mail: Mai-Linh.Doan@obs.ujf-grenoble.fr.

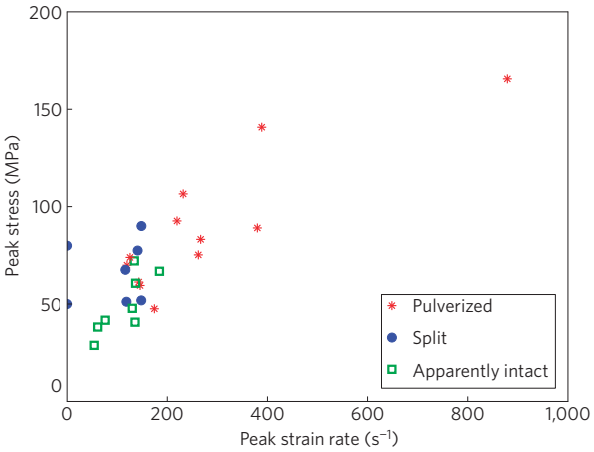

Figure 2 | Experimental results. The final state relative to the peak stress and the peak strain rate. The transition from single crack fracture (blue circles; Fig. 1a) to intense pulverization (red stars; Fig. 1b) depends on strain rate. The threshold occurs between 100 s^{-1} and 150 s^{-1}. Some samples remained unbroken (green squares).

the dependence of our results on the initial damage state, we carried out similar experiments on intact granite samples from Tarn, France (Supplementary Figs S9 and S10). We found a similar transition from sparse fracturing to fragmentation, but at a higher strain rate, about 250 s^{-1}. The fragmentation happens during the first loading (Fig. 3).

Our transition not only delimits different final damage patterns, but also corresponds to an increase in the apparent strength of the sample. These experimental results are in accordance with the statistical theory of Hild[12] for the transition from single to multiple fracturing regimes. In both theory and experiment, rock strength starts to increase with strain rate, once in a pulverization regime. Theoretically, there is an intrinsic increase of the material strength[13], because the propagation of several small fractures requires more energy than that of a single large fracture. Experimentally, the sample does not instantaneously expand laterally at high strain rates, and hence is dynamically confined. When computing the equivalent constraining stress[10], we retrieve dynamic confining pressures in the range of 2–10 MPa, corresponding to a burial depth of only 80–400 m. This suggests that pulverization may also be found in the shallow subsurface, as confirmed by borehole studies[14].

Grain size analyses were carried out on fractured and pulverized rocks (see the Methods section and Supplementary Tables S2 and S3). Most particles have millimetric dimensions, a little larger than the grain size of pulverized rocks[5]. We do not claim to reproduce the exact state of pulverized rocks, especially its grain size distribution. The natural state is certainly the result of several earthquakes, each one damaging rocks by compressional and shear loading waves. Here, we focus only on the transition between localized fracturing and pervasive fragmentation.

We focused on dynamic pulverization to explain pulverization near faults. Other mechanisms may inhibit the strain localization process. One is the ductile–fragile transition at high confining stress or high temperature[15]. However, both parameters are below the transition values (300 MPa, 350 °C; ref. 15) for crystalline rocks at the ground surface. A second way to inhibit strain localization is to apply fast rotating stress. The sheared zones are then reworked over and over, so that the strain localization is annealed at the expense of the formation of preferential microstructure orientation[16]. This mechanism requires large strain, which is not observed in the pulverized rocks from the San Andreas fault because they preserve their original fabric.

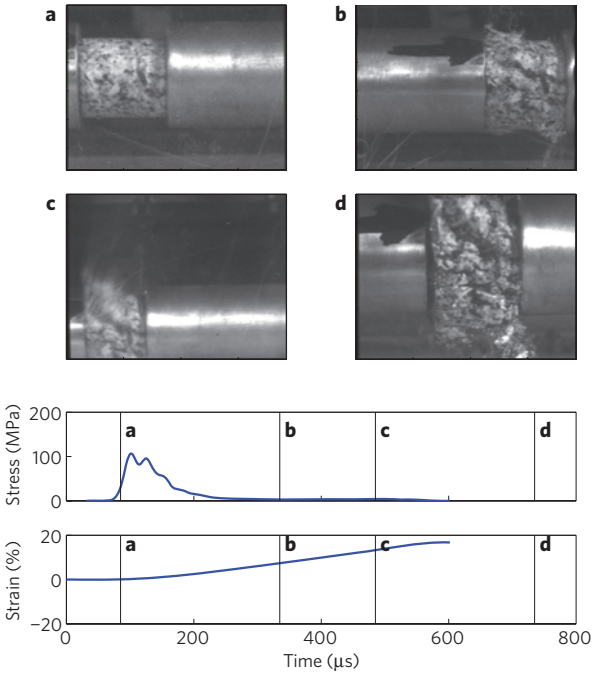

Figure 3 | Time-lapse snapshots of a sample being pulverized. The vertical bars **a**–**d** in the plots at the bottom denote the times corresponding to the photographs, taken with four independently triggered cameras. The measured stress and strain history is reported in the lower graphs. The sample breaks in an early stage (after **a**), but because of their inertia, the fragments fly away later (**b**,**c**,**d**). The sample is fragmented while in compression, and not during stress relaxation.

A high strain rate may be a necessary condition for pulverization, although perhaps not a sufficient condition. Other phenomena can also modulate the onset of pulverization. For instance, rupture along an interface separating material with different elastic moduli can induce tensile loading on only one side[17]. As tensile strength is small, damage is facilitated there. This may explain the asymmetry of damage along faults.

There are also some caveats in relating the laboratory experiments to the field observations. Our experiments were carried out under uniaxial loading. The transition strain rate depends on the speed of fracture propagation and on the interaction between cracks, which are controlled by the statistics of the initial crack population and the size of stress shadow zones around each crack. These parameters do not strongly depend on the fracture mode[18]. The fracture speed propagation is close to the S-wave speed c_S in all fracture modes. The shape of the stressed areas around a crack tip differs with fracture mode, but its size varies similarly, with stress decaying with distance from the fracture tip r as $1/r^{1/2}$. Hence, the transition from single to multiple fracturing is only weakly dependent on the fracture mode[18]. The strain rate condition obtained experimentally is a reasonable approximation to the natural case in that the sample is subject to both shear stress and normal stress.

Figure 2 suggests that the transition from fracturing to pulverization is related to strain rate. An important result of this study is that pulverized rocks appear as markers of high strain rate loading ($>150\,s^{-1}$). This result needs to be evaluated in light of the fact that the initial structure of the pulverized rocks found in the field is preserved, which suggests that the pulverized rocks endured low strain.

To determine the conditions that are required to satisfy the twin constraints of high strain rate but low strain, we computed the strain rate and the stress near a crack tip propagating at a constant velocity. Considering distances from the fault ($r = 100$ m) that are small relative to the rupture size (more than 10 km), we calculate

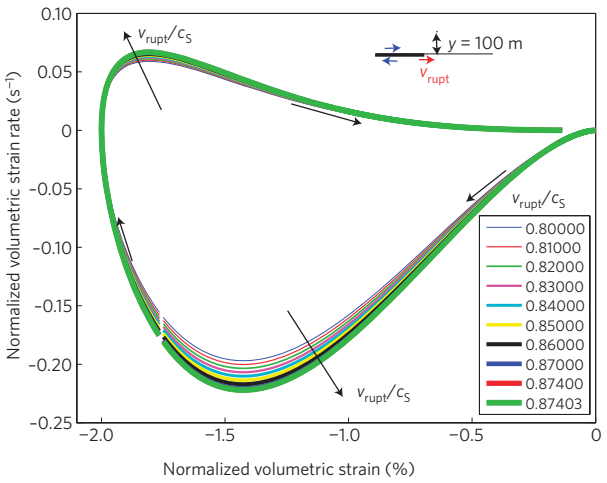

Figure 4 | Dilatational strain rate versus dilatational strain induced by a subshear rupture 100 m from the fault core. We normalized both the strain and strain rate so that the maximum strain amplitude is 2%, corresponding to the order of magnitude of the maximum strain in the pulverized rocks near the San Andreas fault. The curves were computed in plane stress for several rupture speeds, all below the Rayleigh wave speed (here $c_R \sim 0.8740301 c_S$). All curves achieve a maximum strain rate less than 0.25 s^{-1}, three orders of magnitude below our experimental 150 s^{-1} pulverization threshold.

an asymptotic development of stress, dependent on the distance to the rupture tip (see Supplementary Discussion for details of the calculations). The first terms of strain and strain rate for a rupture speed below the S-wave speed (subshear rupture) decay as $1/r^{1/2}$ and $1/r^{3/2}$, respectively[19]. Figure 4 gives the shear strain rate of rocks located 100 m from the fault supposing that the maximum strain is 2%, a value we believe is representative of the maximum strain sustained by the pulverized rocks. The maximum strain rate remains two orders of magnitude below the experimental threshold strain rate permitting pulverization. Other terms of the Taylor expansion of strain[20] give similar or lower strain rates for strains less than 2%. Attaining the experimental threshold is therefore unlikely for subshear rupture in homogeneous material.

In the previous calculation, we made two hypotheses: a homogeneous medium and a subshear rupture. For faults separating two different media, a sharp tensile pulse can be generated in the stiffest part of the fault[21,22]. If the Weertman pulse induces pulverization, we expect to find pulverized rocks along faults separating different materials, with no evidence for compression. However, pulverized sandstone along the San Andreas fault shows compression features[23]. Pulverized rocks are sometimes found on both sides of the San Andreas fault[3]. Hence, we propose that an alternative mechanism, supershear rupture, generates the high strain rate and pulverizes rocks.

Supershear rupture induces a shock wave. Simple models yield Heaviside functions, modelling sharp fronts and with small decay with distance[19] (see Supplementary Discussion for details). High rates of loading can be reached 100 m from the fault core, as supershear rupture induces a shock wave[24] and generates high-frequency displacements[25]. This is consistent with the discovery of pulverized rocks only near large strike-slip faults: San Andreas and San Jacinto faults in California[3,5,23], Northern Anatolia fault in Turkey[26], Arima-Takatsuki fault in Japan[27], which are the most amenable to supershear rupture. We predict that off-fault pulverization should only be found along large strike-slip faults, and this provides a way to test our hypothesis in the future.

This work offers constraints on the formation of pulverized rocks, which endured deformation rates higher than 150 s^{-1}. As possible indicators of previous supershear rupture, and independent of seismological observations, pulverized rocks should therefore be considered in the risk assessment of such potentially damaging earthquakes.

Methods

We experimentally damaged rocks sampled near the pulverized zone at high strain rate, using an SHPB apparatus[8] in the Laboratoire de Mécanique des Solides of the École Polytechnique, Palaiseau, France.

Samples. Samples were collected about 200 m away from the fault core, in the Lake Hughes area (see Supplementary Fig. S5). The rocks were strong enough to be cored. We used this rock material to approximate pulverized rocks as it was before pulverization: the same material, not yet pulverized, but still damaged, as they lay near an active fault.

The samples were taken as boulders in the flanks of a deep gully. As they lay above the bottom of the gully, we assume the boulders were not transported by water, but rather that they fell by gravity from the edges of the gully. The flanks are quite steep, so that the originating outcrops could not be investigated.

Thin sections of the samples (Supplementary Figs S7 and S8) show alteration and dense microfracturing. Hence, we also used samples of Tarn granite, as a supplementary testing. Thin sections in Supplementary Fig. S8 show that the granite is slightly altered but less fractured than the samples from the San Andreas fault.

Experimental device. The experiments were carried out using the device shown in Supplementary Fig. S2. Each sample is inserted between two bars and impacted by a 'striker' arriving with a known speed. The incident stress wave splits into reflected and transmitted waves when it reaches the sample. Incident and reflected waves are measured with a strain gauge on the input bar, and the transmitted wave with a strain gauge on the output bar. Subsequent waves are not recorded as they are superposed at gauge locations and cannot be easily identified.

Processing. Classical processing of the SHPB supposes one-dimensional (1D) propagation of an elastic wave, given the dimensions of the bars (3 m long and 4 cm diameter). Here, we use a very precise measurement of time (with modern data acquisition systems) and a very precise 3D modelling of the wave propagation in bars (based on the Pochhammer and Chree equations) for the computation of forces and displacements at both ends of the specimen. We checked that the forces were identical at the input and output bars, to verify that the sample was homogeneously loaded. Once the quasi-equilibrium of the specimen was verified (equality of input and output forces), we calculated stress, strain and strain rate. A direct measurement of Young's modulus of the specimen is also possible, based on the transient 1D analysis of the test.

Grain size distribution. Some samples were wrapped inside a loose plastic bag attached to the input and output bars of the SHPB apparatus. This allowed us to limit the loss of material during the pulverization of the sample and to conduct grain size analysis (see Supplementary Tables S2 and S3). The grain size distribution of the larger grains was determined by manual sieving by shaking a stack of sieves for 2 min.

Errors in grain size distribution are mainly due to loss of material, which is about 1 g for an initial sample of 25 g. This is also the range of weights measured for each sieve. Hence, the weight of each particle size bin may be underestimated by 100%. Theoretically, all size bins are affected. However, fragmentation experiments produce a large dust cloud that could not be recovered. The contributions of the smallest particles were almost certainly the most underestimated.

Sieving methods measure weight and are biased towards the largest particles, because weight scales as the cube of the particle size. It is therefore difficult to make a quantitative comparison with the natural grain size distribution obtained with a laser granulometer that counts particle number[5]. Still, qualitatively, our grain size is larger than the natural grain size distribution of pulverized rocks, but smaller than the original grain size of our samples.'

Modal analysis. We carried out modal analysis of two thin sections drilled within a sample taken near Lake Hughes outcrop (see Supplementary Fig. S5), and one thin section drilled within a sample of Tarn granite. The modal analysis of each thin section was conducted by identifying the mineral located at 315 random points within the thin section. The error estimation can be quantified using the central limit theorem[28]. If a mineral is found n times for N point counts, the upper limit of the 95% confidence interval is computed as

$$P^u = 100 * \beta(1-\alpha, n+1, N-n)$$

where $\alpha = 1$–0.95 and β is the inverse of the beta cumulative distribution function. The lower bound of the 95% confidence interval is computed as

$$P_l = 100 * [1-\beta(1-\alpha, N-n+1, n)]$$

Received 18 February 2009; accepted 27 August 2009; published online 27 September 2009

References

1. Caine, J. S., Evans, J. P. & Forster, C. B. Fault zone architecture and permeability structure. *Geology* **24,** 1025–1028 (1996).
2. Chester, F. M., Evans, J. P. & Biegel, R. L. Internal structure and weakening mechanisms of the San Andreas fault. *J. Geophys. Res.* **98,** 771–786 (1993).
3. Dor, O., Ben-Zion, Y., Rockwell, T. K. & Brune, J. N. Pulverized rocks in the Mojave section of the San Andreas fault zone. *Earth Planet. Sci. Lett* **245,** 642–654 (2006).
4. Wilson, B., Dewers, T., Reches, Z. & Brune, J. Particle size and energetics of gouge from earthquake rupture zones. *Nature* **434,** 749–752 (2005).
5. Rockwell, T. K. *et al*. Granulometric and mineralogical properties of pulverized rocks from Tejon Pass on the San Andreas fault and from Tejon Ranch on the Garlock fault, California. *Pure Appl. Geophys.* (in the press).
6. Grady, D. E. & Kipp, M. E. in *Fracture Mechanics of Rocks* (ed. Atkinson, B. E.) (Academic, 1989).
7. Reches, Z. & Dewers, T. A. Gouge formation by dynamic pulverization during earthquake rupture. *Earth. Planet. Sci. Lett.* **235,** 361–374 (2005).
8. Kolsky, H. *Stress Waves in Solids* (Dover Publications, 1963).
9. Zhao, H. & Gary, G. On the use of SHPB techniques to determine the dynamic behavior of materials in the range of small strains. *Int. J. Solids Struct.* **33,** 3363–3375 (1996).
10. Forrestal, M. J., Wright, T. W. & Chen, W. The effect of radial inertia on brittle samples during the split Hopkinson pressure bar test. *Int. J. Impact Eng.* **34,** 405–411 (2007).
11. Lide, D. R. (ed.) in *CRC Handbook of Chemistry and Physics: A Ready-Reference Book of Chemical and Physical Data* 88th edn (Boca Raton, 2008).
12. Hild, F., Forquin, P. & Cordeiro da Silva, A. R. Single and multiple fragmentation of brittle geomaterials. *Rev. Franco. Gen. Civ.* **7,** 973–1003 (2003).
13. Li, Q. M. & Meng, H. About the dynamic strength enhancement of concrete-like materials in a split Hopkinson pressure bar test. *Int. J. Solids Struct.* **40,** 343–360 (2003).
14. Wechsler, N., Allen, E. E., Rockwell, T. K., Chester, J. & Ben-Zion, Y. Characterization of pulverized granite from a traverse and a shallow drill along the San Andreas fault, Little Rock, CA. *Seismological Society of America Annual Meeting, Seismol. Res. Lett.* **80,** 319 (2009).
15. Guéguen, Y. & Palciauskas, V. *Introduction to the Physics of Rocks* (Princeton Univ. Press, 1994).
16. Bystricky, M., Kunze, K., Burlini, L. & Burg, J. P. High shear strain of olivine aggregate: Rheological and seismic consequences. *Science* **290,** 1564–1567 (2000).
17. Ben Zion, Y. & Andrews, D. J. Properties and implication of dynamic rupture along a material interface. *Bull. Seismol. Soc. Am.* **88,** 1084–1094 (1998).
18. Huang, C., Subhash, G. & Vitton, S. J. A dynamic damage growth model for uniaxial compressive response of rock aggregates. *Mech. Mater.* **34,** 267–277 (2002).
19. Freund, L. B. *Dynamic Fracture Mechanics* (Cambridge Univ. Press, 1990).
20. Xu, Y. & Keer, L. M. Higher order asymptotic field at the moving crack tip. *Int. J. Fracture* **58,** 325–343 (1992).
21. Ben-Zion, Y. Dynamic ruptures in recent models of earthquake faults. *J. Mech. Phys. Solids* **49,** 2209–2244 (2001).
22. Andrews, D. J. & Ben-Zion, Y. Wrinkle-like slip pulse on a fault between different materials. *J. Geophys. Res.* **102,** 553–571 (1997).
23. Dor, O., Chester, J. S., Ben-Zion, Y., Brune, J. N. & Rockwell, T. K. Characterization of damage in sandstones along the Mojave section of the San Andreas Fault: Implications for the shallow extent of damage generation. *Pure Appl. Geophys.* **166,** doi:10.1007/s00024-009-0516-z (2009).
24. Rosakis, A., Samudrala, O. & Coker, D. Cracks faster than the shear wave speed. *Science* **284,** 1337–1340 (1999).
25. Bizarri, A. & Spudich, P. Effects of supershear rupture speed on the high-frequency content of S waves investigated using spontaneous dynamic rupture models and isochrone theory. *J. Geophys. Res.* **113,** B05304 (2008).
26. Dor, O. *et al*. Geological and geomorphologic asymmetry across the rupture zones of the 1943 and 1944 earthquakes on the North Anatolian fault: Possible signals for preferred earthquake propagation direction. *Geophys. J. Int.* **173,** 483–504 (2008).
27. Mitchell, T. M., Shimamoto, T. & Ben-Zion, Y. Pulverized fault rocks along the Arima-Takatsuki Tectonic line, Japan: Fault structure, damage distribution and textural characteristics. *EGU General Assembly, Geophys. Res. Abstr.* **11,** EGU2009-11751-2 (2009).
28. Howarth, R. J. Improved estimators of uncertainty in proportions, point-counting, and pass-fail test results. *Am. J. Sci.* **298,** 594–607 (1998).

Acknowledgements

We thank R. Barre, C. Rousseau, J.-B. Toni, R. Leau and R. Guiguet for their technical help and F. Hild, K. Safa, M. Bouchon and P. Favreau for discussions on this paper; V. D'Hour made preliminary work on Tarn granite. We thank E. Brodsky, F. Renard, J.-P. Gratier, Y. Ben-Zion, S. Boutareaud, P. Molnar and R. Hellmann for reading previous drafts of this manuscript. This work was financially supported by the 3F INSU/CNRS program and by the PPF 'Systèmes Complexes' of the University Joseph Fourier.

Author contributions

M.L.D. proposed and participated in the experiments, processed the data and made the computations. M.L.D. also made the grain size distribution measurements and modal analysis. G.G. developed the SHPB apparatus at the École Polytechnique and was in charge of the experiments.

Additional information

Supplementary information accompanies this paper on www.nature.com/naturegeoscience. Reprints and permissions information is available online at http://npg.nature.com/reprintsandpermissions. Correspondence and requests for materials should be addressed to M.L.D.